Growth and Electronic Properties of Ag Overlayers on Stepped Pt(211) Surface

Yu Kwon Kim, Jeong Won Kim, and Sehun Kim*

Department of Chemistry and Center for Molecular Science
Korea Advanced Institute of Science and Technology, Taejon 305-701, Korea
Received October 4, 1996

The growth and electronic properties of ultrathin silver films deposited onto Pt(211) surface were studied using Auger electron spectroscopy (AES), low-energy electron diffraction (LEED), and x-ray photoelectron spectroscopy. The AES and LEED results indicate that the silver grows by a layer by layer growth followed by three dimensional islands growth. The XPS results show that the Ag 3d core-level binding energy of Ag overlayers on Pt(211) shifts toward lower binding energy relative to the bulk value at lower Ag coverage. This negative binding energy shift of the Ag 3d core level is explained by the reduced coordination number of the overlayer atoms and the resulting initial state band narrowing effect suggested by Wertheim and Citrin [Phys. Rev. Lett. **1978**, 41, 1425].

Introduction

The epitaxial growth of metal thin films on metal substrates has been a topic of much interest because of the prospects for versatile applications to new catalysts, magneto-optic films, and corrosion protective films for the last decades.[1~3] Recently, the role of steps on the solid surfaces is especially of major importance for the crystal growth and catalytic process. For example, the stepped surfaces have been successfully used as a template to grow quantum wires with the molecular beam epitaxy technique.[4]

The surface properties of metal overlayers on metal system are remarkably different from those of the constituents in a bimetallic system. The properties of the metal overlayers on metal system can be elucidated by understanding the microscopic structures of the initial growth of the overlayers. Therefore, much research efforts have been devoted to reveal the electronic structure of the metal overlayers on metal system as well as those nanostructures.

Silver overlayers on platinum substrate have been studied as a model system of the catalysts that are used in hydrocarbon conversion reaction.[5~7] The Ag/Pt bimetallic system has shown higher reactivity and selectivity than the Pt catalyst for this reaction. The surface properties of Ag overlayers on the Pt surface have been investigated by using various surface science techniques: thermal desorption spectroscopy (TDS),[8~9] thermal energy He-atom scattering (TEAS),[10~12] scanning tunneling microscopy (STM),[13~14] ultraviolet and/or x-ray photoemission spectroscopy (UPS, XPS).[15~20]

In this work, we employed XPS, low energy electron diffraction (LEED), and Auger electron spectroscopy (AES) as the techniques for elucidating the growth and electronic structures of the Ag overlayers on the highly stepped Pt(211) substrate.

Experiment

The experiments were performed in a Perkin-Elmer UHV chamber equipped with LEED, AES, and XPS spectrometer. The base pressure of the UHV system was maintained at less than 2.0×10^{-10} torr. The Pt(211) sample was cleaned by repeated cycles of sputtering and annealing. The trace of carbon left was removed by annealing the sample at the O_2 atmosphere of 5.0×10^{-8} torr and final flashing at 1270 K. The amount of carbon determined by AES was below detection limit of the instrument and the clear LEED pattern of Pt(211) was obtained.

Silver was deposited on the Pt(211) crystal at room temperature by using a 0.25 mm diameter tantalum wire heater wrapped with a silver wire. The AES and XPS spectra were recorded with the Perkin-Elmer ESCA/AES system with a cylindrical mirror analyzer. The x-ray source used was an Al-Kα line with 160-W power. The Ag 3d core-level binding energies were calibrated by referencing the binding energy of Pt 4*f* core level. The AES measurements were used to characterize the coverage and growth mode of the Ag on Pt(211) surface.

Results and Discussion

Figure 1 shows a plot of the Auger signal versus Ag deposition time (AS-t) for the Pt(211) surface. The Auger peak to peak intensities of Ag(351eV) and Pt(64eV) were normalized as follows.

$$I_{norm}(\mathrm{Pt})=\frac{I_{\mathrm{Pt}}(64\mathrm{eV})}{I_{\mathrm{Pt}}(64\mathrm{eV})+I_{\mathrm{Ag}}(351\mathrm{eV})}$$

$$I_{norm}(\mathrm{Ag})=\frac{I_{\mathrm{Ag}}(351\mathrm{eV})}{I_{\mathrm{Pt}}(64\mathrm{eV})+I_{\mathrm{Ag}}(351\mathrm{eV})}$$

Also drawn are the lines which represent the theoretically calculated intensities of Ag(351eV) and Pt(64eV) with the assumption of a layer by layer growth mechanism using the following formula.

$$I_{\mathrm{Pt}}(64\mathrm{eV})=I_{\mathrm{Pt}}{}^{0}(64\mathrm{eV})\ e^{-d/\lambda_{\mathrm{Pt}}}$$

$$I_{\mathrm{Ag}}(351\mathrm{eV})=I_{\mathrm{Ag}}{}^{0}(351\mathrm{eV})\ (1-e^{-d/\lambda_{\mathrm{Ag}}})$$

where d is the thickness of the overlayer and λ_{Pt} and λ_{Ag}

*corresponding author

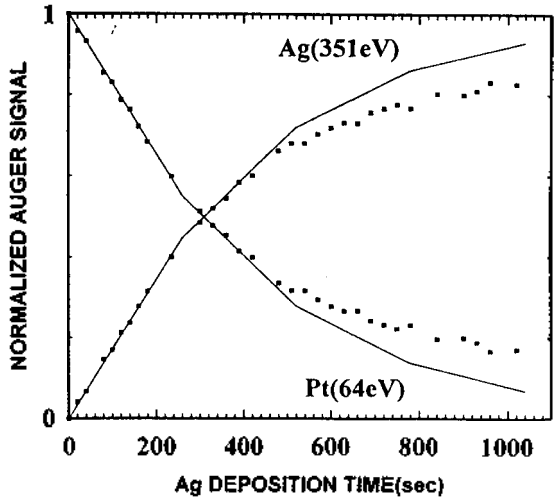

Figure 1. The plot of normalized Auger peak to peak intensities (Pt: 64 eV, Ag: 351 eV) as a function of deposition time of Ag deposited on the Pt(211) surface at room temperature. Initial straight lines were calculated with the inelastic mean free path of electron: λ_{IMFP}(64 eV)=3.6 Å and λ_{IMFP}(351 eV)=7.2 Å.

are the values of the inelastic mean free paths of Pt and Ag respectively.

The values of the inelastic mean free path of the electron calculated at the kinetic energy of 64 eV and 351 eV were 3.6 Å and 7.2 Å, respectively, which are consistent with the previous calculations.[21] The normalized Pt Auger signal decreases rapidly with increasing Ag evaporation time and then converges to a saturation value. The Ag Auger signal increases linearly up to about 260 s evaporation time and then varies smoothly with Ag deposition time. The AS-t plot for Ag and Pt show a break point in the slope at about 260 s deposition time. The observed break point at which the change of the slope in the AS-t plot is located is interpreted to be associated with the completion of one monolayer of atoms on the flat surface. Then, the break point at 260 s deposition time can be assigned as one monolayer coverage of Ag on the Pt(211) surface. After 260 s deposition time, the plot shows a smooth variation in the slope with increasing the deposition time. These results imply that after a completion of approximately one monolayers of Ag atoms on the Pt surface the Ag atoms aggregates into three dimensional islands. We may then conclude that the growth mode of this system follows a layer by layer growth followed by three dimensional islands growth, so called Stranski-Krastanov mode.[22~24] Recently, Bauer *et al.* reported that at a submonolayer coverage the break points in the AS-t plot may occur due to the influence of misfit or strain.[25~26] When the metal such as Fe or Co is deposited on Mo(110) substrate, it is reported that the structural phase transitions which might cause the break point in the AS-t plot occur at the submonolayer coverage. However, we may rule out this possibility since the lattice mismatch of Ag/Pt system is relatively smaller than that of Fe/Mo or Co/Mo. Also we observed that the 1×1 LEED pattern were maintained up to the coverage of 4 ML, which indicates that the structural changes at the submonolayer coverage unlikely occurred.

The clean Pt(211) surface shows a characteristic 1×1

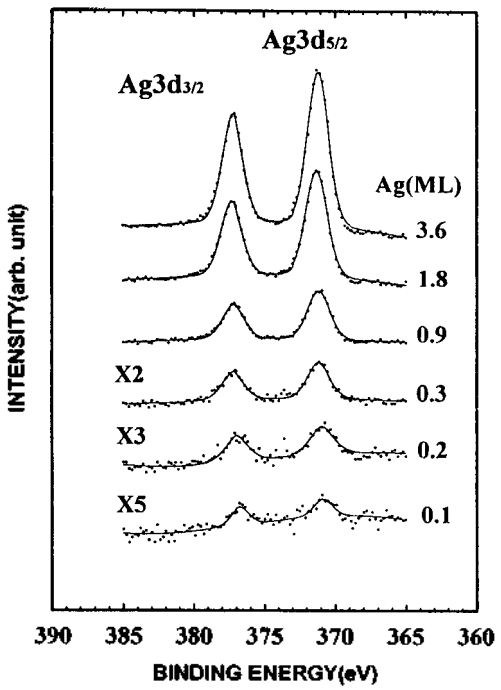

Figure 2. X-ray photoelectron spectra of Ag 3d core levels for Ag adlayers deposited on Pt(211) with θ=0.1, 0.2, 0.3, 0.9, 1.8, and 3.6 ML.

LEED pattern corresponding to the monoatomic height step-terrace 3(111)×(100) plane.[27~29] Upon the deposition of Ag up to the coverage of 0.3 ML, the intensities of the sharp integer spots decrease drastically. This means that the long-range ordered Pt(211) surface becomes covered with the randomly distributed Ag islands of a few angstrom. As silver was more evaporated on the Pt surface, a sharp commensurate 1×1 LEED pattern was rapidly recovered and preserved up to 1 ML Ag coverage with a relative intensity change of the LEED spots. This indicates that the small Ag islands aggregate to form even larger islands upon the deposition of Ag more than 0.3ML and these 2-dimensional islands with a domain larger than the coherent length of the electron of the LEED electron gun are preserved up to 1ML.[30~31] Upon depositing more than 1 ML the LEED spots were maintained with slight increase in the diffuse background up to 3 ML coverage. This is the result of the increase of the surface roughness, that is, the transformation of the 2-dimensional Ag islands into the 3-dimensional ones. This result is consistent with the above AES measurement, suggesting a Stranski-Krastanov growth.

Figure 2 shows x-ray photoelectron spectra of Ag 3d core levels at silver coverages from 0.1 to 3.6 ML. In order to determine accurate positions, a curve fitting to the Ag 3d core level spectra was performed by the convolution of Lorentzian function and Gaussian function due to instrumental line broadening. The involved parameters in the fitting procedure are the intensity ratio of the spin-orbit splitting of Ag 3d core level together with its binding energy, Lorentzian line width, asymmetry parameter, and Gaussian broadening. The Gaussian width due to the instrumental broadening was estimated to be 1.6± 0.1 eV. The asymmetry parameter was fixed to 0.03.[32] The spin-orbit splitting energy between Ag

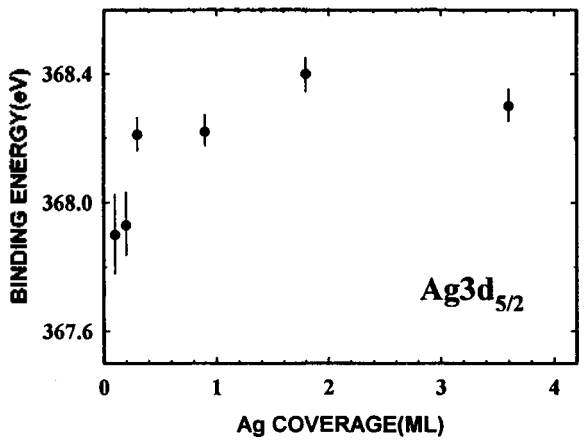

Figure 3. The binding energies of the Ag $3d_{5/2}$ core level as a function of the Ag coverage.

$3d_{5/2}$ and Ag $3d_{3/2}$ varied from 6.17 eV at $\theta=3.6$ ML to 6.0 eV at the lowest coverage. The measured $Ag(3d_{3/2})/Ag(3d_{5/2})$ intensity ratio is 0.7 at $\theta=3.6$ ML and somewhat higher at lower coverages. Figure 3 presents the plot of the binding energies of the Ag $3d_{5/2}$ core level versus the Ag coverage. The observed binding energy of the Ag 3d core level is 367.9 eV at 0.1 ML Ag coverage. The binding energy shifts to 368.2 eV at 0.3 ML coverage and then flattens at higher coverages. Since the Gaussian width variation was lower than 0.1 eV, the observed binding energy shift can be regarded as the surface core level shift of deposited Ag atoms at the Ag coverages lower than 0.3 ML. The error bars in Figure 3 were determined by allowing the deviations of the fitting parameters within 70% confidence limit.

The observed shift to higher binding energy of the Ag 3d core level with increasing the Ag coverage (the increase of the Ag cluster size) [Figure 3] can be interpreted by an initial state band narrowing effect of the surface atoms in the noble metals suggested by Wertheim and Citrin.[33~39] According to their model, the surface atoms have fewer neighboring atoms than the bulk atoms. The reduced coordination number of atoms on the surface compared to the bulk atoms results in a narrowing of the surface valence band. In the Ag case, this is achieved by a combined reduction of d delocalization and s-d hybridization, giving an overall net increase in the localized d states at the expense of the delocalized d states. The resulting band narrowing effect is to lower the Fermi level of the surface bands below that of the bulk bands. In order to restore equilibrium and bring the Fermi level back into coincidence, a small amount of charge must flow into the surface bands. The Coulomb potential of this charge raises the energy of both the surface valence band and the core levels by comparable amounts. We therefore expect that this lower binding energy shift, so-called the negative shift, of the core level binding energy of the surface atoms compared to the bulk atoms has been observed for elemental noble metals.[41] The similar negative shift of the core level binding energy of the overlayer atoms on the metal substrate has been reported for some bimetallic system such as Au/Pt(100),[15] Cu/Rh(100),[43] Ni/Ru(0001),[43] Pd/Pt(111)[42] and Ni/Cu(100).[44~47] For the Au/Pt(100) system, Salmerón *et al.* explained the negative binding energy shift of Au 4f level as due to the different contribution of the Au atoms in islands edges for surface and bulk coordination positions.[15] The number of edge atoms in the Au overlayers increases with decreasing the Au coverage. The edge atoms with the reduced coordination number and the resulting narrow band width are responsible for the negative binding energy shift at the lower coverage. Similarly, the observed negative binding energy shift of the Ag core level on Pt(211) surface at the lower Ag coverage can be understood by the reduced coordination number of the overlayer atoms and the resulting band narrowing effect. This result is consistent with the interpretation of our LEED observations at the Ag coverage less than 0.3 ML.

Conclusions

AES and LEED results suggest that the silver grows in a two dimensional layer on the terrace of the Pt(211) plane below one monolayer (ML) coverage followed by the growth of three dimensional islands at higher coverages. The LEED observation confirmed that the Ag grows commensurately on the Pt(211) surface. Moreover, it also revealed that the Ag islands of a few angstrom wide are randomly distributed on this surface when the coverage is lower than 0.3 ML. The XPS results show that the Ag 3d core-level binding energy of Ag overlayers on Pt(211) shifts toward lower binding energy relative to the bulk value at lower Ag coverage. The negative binding energy shift of the Ag 3d core level is due to the reduced coordination number of the overlayer atoms and the resulting initial state band narrowing effect suggested by Wertheim and Citrin.[33~35] Combined with the LEED results, this negative binding energy shift below 0.3 ML Ag coverage also supports that the Ag atoms start to grow as small islands at this coverage and grow as the large two dimensional islands on the terrace sites of the Pt(211) surface above 0.3 ML Ag coverage.

References

1. Rodriguez, J. A.; Goodman, D. W. *Surf. Sci. Rep.* **1991**, *14*, 1.
2. Kern, R.; Le Lay, G.; Metois, J. J. *Current Topics in Materials Science*; Kaldis, E. Ed.; North-Holland, Amsterdam, 1979; vol. 3, p 131.
3. Santra, A. K.; Rao, C. N. R. *J. Phys. Chem.* **1994**, *98*, 5962.
4. (a) Petroff, P. M.; Gossard, A. C.; Wiegmann, W. *Appl. Phys. Lett.* **1984**, *45*, 620. (b) Miller, M. S.; Weman, H.; Pryor, C. E.; Krishnamurthy, M.; Petroff, P. M.; Kroemer, H.; Merz, J. L. *Phys. Rev. Lett.* **1992**, *68*, 3464.
5. Ponec, V. *Catalysis Rev. Sci. Eng.* **1970**, *11*, 41.
6. Ponec, V. *Surf. Sci.* **1979**, *80*, 352.
7. Sachtler, W. M. H. *Catalysis Rev. Sci. Eng.* **1976**, *14*, 193.
8. Shern, C. S.; Chang, D. U.; Syru, K. D.; Tsay, J. S.; Fu, Tsu-yi *Surf. Sci.* **1994**, *318*, 262.
9. Davies, P. W.; Quinlan, M. A.; Somorjai, G. A. *Surf. Sci.* **1982**, *121*, 290.
10. Becker, A. F.; Rosenfeld, G.; Poelsema, B.; Comsa, G. *Phys. Rev. Lett.* **1993**, *70*, 477.
11. Poelsema, B.; Becker, A. F.; Rosenfeld, G.; Kunkel, R.; Nagel, N.; Verheij, L. K.; Comsa, G. *Surf. Sci.* **1992**, *272*,

269.
12. Blandin, P.; Massobrio, C.; Ballone, P. *Phys. Rev. Lett.* **1994**, *72*, 3072.
13. Röder, H.; Brune, H.; Bucher, J.-P.; Kern, K. *Surf. Sci.* **1993**, *298*, 121.
14. Röder, H.; Schuster, R.; Brune, H.; Kern, K. *Phys. Rev. Lett.* **1993**, *71*, 2086.
15. Salmerón, M.; Ferrer, S.; Jazzar, M.; Somorjai, G. A. *Phys. Rev. B* **1983**, *28*, 6758.
16. Eyers, A.; Schäfers, F.; Schönhense, G.; Heinzmann, U.; Oepen, H. P.; Hünlich, K.; Kirschner, J.; Borstel, G. *Phys. Rev. Lett.* **1984**, *52*, 1559.
17. Schmiedeskamp, B.; Kessler, B.; Vogt, B.; Heinzmann, U. *Surf. Sci.* **1989**, *223*, 465.
18. Paffett, M. T.; Campbell, C. T.; Taylor, T. N. *Langmuir* **1985**, *1*, 741.
19. Mason, M. G.; Baetzold, R. C. *J. Chem. Phys.* **1976**, *64*, 271.
20. Apai, G.; Lee, S.-T.; Mason, M. G. *Sol. Stat. Comm.* **1981**, *37*, 213.
21. Palmberg, P. W.; Rhodin, T. N. *J. Appl. Phys.* **1968**, *39*, 2425.
22. Argile, C.; Rhead, G. E. *Surf. Sci. Rep.* **1989**, *10*, 277.
23. Paffett, M. T.; Windham, R. G. *Surf. Sci.* **1989**, *208*, 34.
24. Bauer, E. *Appl. Surf. Sci.* **1982**, *11/12*, 479.
25. Van der Merwe, H.; Bauer, E. *Phys. Rev. B* **1989-II**, *39*, 3632.
26. Tikhov, M.; Bauer, E. *Surf. Sci.* **1990**, *232*, 73.
27. Blakely, D. W.; Somorjai, G. A. *Surf. Sci.* **1977**, *65*, 419.
28. Roberts, R. H.; Pritchard, J. *Surf. Sci.* **1976**, *54*, 687.
29. Chesters, M. A.; Hussain, M.; Pritchard, J. *Surf. Sci.* **1973**, *35*, 161.
30. Paffett, M. T.; Campbell, C. T.; Taylor, T. N.; Srinivasan, S. *Surf. Sci.* **1985**, *154*, 284.
31. Flynn, D. K.; Evans, J. W.; Thiel, P. A. *J. Vac. Sci. Technol. A* **1989**, *7*, 2162.
32. Citrin, P. H.; Wertheim, G. K.; Baer, Y. *Phys. Rev. B* **1977**, *16*, 4256.
33. Citrin, P. H.; Wertheim, G. K.; Baer, Y. *Phys. Rev. Lett.* **1978**, *41*, 1425.
34. Citrin, P. H.; Wertheim, G. K.; Baer, Y. *Phys. Rev. B* **1983**, *27*, 3160.
35. Citrin, P. H.; Wertheim, G. K. *Phys. Rev. B* **1983**, *27*, 3176.
36. Steiner, P.; Hüfner, S. *Sol. Stat. Comm.* **1981**, *37*, 279.
37. Mårtensson, N.; Stenborg, A.; Björneholm, O.; Nilsson, A.; Andersen, J. N. *Phys. Rev. Lett.* **1988**, *60*, 1731.
38. Johansson, B.; Mårtensson, N. *Phys. Rev. B* **1980**, *21*, 4427.
39. Tománek, D.; Kumar, V.; Holloway, S.; Bennemann, K. H. *Sol. Stat. Comm.* **1982**, *41*, 273.
40. Nilsson, A.; Eriksson, B.; Mårtensson, N.; Andersen, J. N.; Onsgaard, J. *Phys. Rev. B* **1988-II**, *38*, 10357.
41. Derry, G. N. *Surf. Sci.* **1994**, *316*, L1044.
42. Han, M.; Mrozek, P.; Wieckowski, A. *Phys. Rev. B* **19 93-I**, *48*, 8329.
43. Rodriguez, J. A.; Campbell, R. A.; Goodman, D. W. *J. Phys. Chem.* **1990**, *94*, 6936.
44. Egelhoff, W. F. Jr. *J. Vac. Sci. Technol. A* **1983**, *1*, 1102.
45. Hernnäs, B.; Karolewski, M.; Tillborg, H.; Nilsson, A.; Mårtensson, N. *Surf. Sci.* **1994**, *302*, 64.
46. Yang, S.; Yu, M.; Meigs, G.; Feng, X. H.; Garfunkel, E. *Surf. Sci.* **1988**, *205*, L777.
47. Campbell, R. A.; Rodriguez, J. A.; Goodman, D. W. *Surf. Sci.* **1991**, *256*, 72.